SRSF protein kinases 1 and 2 are essential host factors for human coronaviruses including SARS-CoV-2

Brook E. Heaton*[1], Joseph D. Trimarco[1], Cait E. Hamele[1], Alfred T. Harding[1], Aleksandra Tata[2], Xinyu Zhu[1], Purushothama Rao Tata[2,3,4], Clare M. Smith[1,5], and Nicholas S. Heaton[1,3,5]*

[1] Department of Molecular Genetics and Microbiology, Duke University School of Medicine, Durham, North Carolina, USA, 27710

[2] Department of Cell Biology, Duke University School of Medicine, Durham, North Carolina, USA, 27710

[3] Duke Cancer Institute, Duke University School of Medicine, Durham, NC 27710, USA

[4] Regeneration Next, Duke University, Durham, NC 27710, USA

[5] Duke Human Vaccine Institute, Duke University School of Medicine, Durham, North Carolina, USA, 27710

*to whom correspondence should be addressed

Brook E. Heaton
Research Assistant Professor
Department of Molecular Genetics and Microbiology (MGM)
Duke University School of Medicine
213 Research Drive, 427 CARL Building, Box 3054
Durham, NC 27710
Email: brook.heaton@duke.edu

Nicholas S. Heaton
Assistant Professor
Department of Molecular Genetics and Microbiology (MGM)
Duke University School of Medicine
213 Research Drive, 426 CARL Building, Box 3054
Durham, NC 27710
Email: nicholas.heaton@duke.edu

ABSTRACT

Antiviral therapeutics against SARS-CoV-2 are needed to treat the pandemic disease COVID-19. Pharmacological targeting of a host factor required for viral replication can suppress viral spread with a low probability of viral mutation leading to resistance. Here, we performed a genome-wide screen in human lung epithelial cells to identify potential host therapeutic targets. We report that the kinase SRPK1, together with the closely related SRPK2, are jointly essential for SARS-CoV-2 replication; inhibition of SRPK1/2 with small molecules led to a dramatic decrease (more than 100,000-fold) in SARS-CoV-2 virus production in immortalized and primary human lung cells. Subsequent biochemical studies revealed that SPRK1/2 phosphorylate the viral nucleocapsid (N) protein at sites highly conserved across human coronaviruses and, due to this conservation, even a distantly related coronavirus was highly sensitive to an SPRK1/2 inhibitor. Together, these data suggest that SRPK1/2-targeted therapies may be an efficacious strategy to prevent or treat COVID-19 and other coronavirus-mediated diseases.

INTRODUCTION

In December 2019, a novel human coronavirus, now known as SARS-CoV-2, emerged and began causing a human disease termed COVID-19[1,2]. Since then, a global pandemic has infected millions and caused hundreds of thousands of deaths to date. Due to the prevalence and severity of this disease, the development of therapeutic interventions is of the highest importance. Much attention has been focused on targeting viral proteins and their associated enzymatic activities. In particular, the virally encoded RNA-

67 dependent RNA polymerase (RdRp) and the viral proteases, are attractive potential
68 targets. Remdesivir, the only FDA-approved antiviral for SARS-CoV-2, is a nucleoside
69 analogue which targets the viral RdRp and causes premature termination of
70 transcription[3]. Efficacy of this treatment however, unfortunately, appears limited[4].
71
72 In addition to targeting viral proteins directly, other antiviral development strategies
73 attempt to target host factors that the virus requires to complete its lifecycle. Relative to
74 their hosts, viruses have dramatically less coding space in their genomes and therefore
75 utilize host proteins to supplement the activities of their own proteins. The major
76 advantages of inhibiting a virus indirectly via an essential host factor are two-fold: (1)
77 many viruses may utilize the same host protein, therefore host-directed therapeutics have
78 the potential to be broadly acting and (2) while direct targeting of the virus can rapidly
79 select for resistant viral mutants, it is thought to be much more difficult for a viral mutation
80 to overcome inhibition of a co-opted host protein.
81
82 The development of host-directed COVID-19 therapeutics has been hindered however,
83 due to an incomplete understanding of the host factors required for SARS-CoV-2
84 replication; this is in no small part due to its recent emergence into the human population.
85 While a CRISPR/Cas9 screen for the host factors utilized by SARS-CoV-2 in African
86 green monkey cells (*Chlorocebus sp.*) was recently reported[5], we chose to perform an
87 independent screen in the human lung epithelial cell line (A549) ectopically over-
88 expressing the SARS-CoV-2 receptor ACE2. Although incomplete viral cytopathic effect
89 in our cell line led to only limited enrichment of host factors, pharmacological targeting of

90 our top hit, SRSF Protein Kinase 1 (SPRK1) and the highly related SRPK2, strongly
91 inhibited the replication of both human alpha- and beta-coronaviruses. This inhibition was
92 likely due to altered phosphorylation of the respective viral nucleocapsid proteins. Thus,
93 not only are the enzymatic activities of SRPK1/2 essential for the replication of multiple
94 human coronaviruses, but targeting these kinases may represent an effective therapeutic
95 approach for coronavirus mediated diseases, including COVID-19.
96
97 **RESULTS**
98 While CRISPR/Cas technology allows most known genes in the host genome to be
99 rapidly screened for effects on viral replication, efficient viral killing of the cells with
100 irrelevant genetic modifications is required. Unfortunately, SARS-CoV-2 cytopathic
101 effects have been reported to be mostly restricted to cell lines derived from non-human
102 primates, which precludes efficient screening in human cell lines[6]. In an attempt to
103 overcome this limitation, we generated lentiviruses harboring the SARS-CoV-2 receptor
104 ACE2, and stably transduced (at high MOI) a human A549 lung epithelial cell clone that
105 had already been engineered to express Cas9 from *Streptococcus pyogenes*. This cell
106 line expressed ~100x more ACE2 than the parental line, and was drastically more
107 permissive to SARS-CoV-2 infection. Cellular killing by SARS-CoV-2, while improved,
108 was still incomplete (**Supplemental Figure 1**).
109
110 In order to test if this experimental system could enrich for human host factors critical for
111 SARS-CoV-2 infection, $2x10^7$ A549-Cas9-ACE2 cells (in two biological replicates) were
112 transduced at a multiplicity of infection (MOI) of 0.8 with lentiviruses harboring the GeCKO

113 V2 sgRNA library A. This library contains three individual sgRNAs against most annotated
114 genes in the human genome[7]. Five days post-transduction, a timepoint after which
115 genome editing and protein turnover has occurred, half of the cells ($6x10^7$ cells/replicate)
116 were infected with SARS-CoV-2 at an MOI of 0.05 followed by multicycle viral growth for
117 72 hours. The remaining half of the cells were collected as an unselected comparison.
118 After collection (and expansion) of the cells rendered refractory to viral infection by
119 CRISPR targeting, we sequenced the sgRNAs from both the input and post-selection
120 samples (**Figure 1A, Supplemental Dataset 1**).
121
122 Due to incomplete viral killing of our A549 cell line, we detected many of the input sgRNAs
123 (and limited enrichment of any particular sgRNA) in our post-selection population
124 **(Supplemental Dataset 2)**. Despite the limited dynamic range, statistical analysis[8] of the
125 sgRNA sequencing data indicated that the host gene with the highest probability of being
126 required for SARS-CoV-2 infection was the serine/arginine-rich protein kinase, SRPK1
127 (**Figure 1B**). We did not enrich for ACE2, presumably due to the numerous lentivirus-
128 integrated copies of ACE2 causing inefficient targeting in our cell line. We chose to move
129 forward by interrogating potential roles for SRPK1 during viral infection as kinases are
130 generally thought to be good drug targets[9], and identifying drug targets was the initial goal
131 of our screen. Since a number of SARS-CoV-2 proteins have been reported to be
132 phosphorylated, we took a bioinformatic approach to predict potential SRPK1
133 phosphorylation sites[10] across the entire SARS-CoV-2 genome (**Figure 1C,**
134 **Supplemental Table 1**). The viral protein with by far the highest confidence predicted
135 SRPK1 sites was the viral nucleoprotein (N). Phosphoproteomic studies of SARS-CoV-

136 2 proteins have reported that some of the predicted SRPK1 phosphorylation sites in the
137 N protein are indeed phosphorylated[11-13] (**Fig 1C**). We therefore hypothesized that
138 SRPK1 was likely responsible for the phosphorylation of at least some sites in the N
139 protein.
140
141 We next wanted to define the degree to which inhibition of SRPK1 mediated N
142 phosphorylation would affect viral replication, especially since other non-SRPK1 kinases
143 have been predicted to be responsible for SARS-CoV-2 protein phosphorylation[12,13]. We
144 selected the SRPK1 inhibitor SPRIN340 (**Figure 1D**) as it has been reported to inhibit
145 SRPK1 (and SRPK2 with an ~10x higher IC50) without affecting other kinases including
146 the related serine/arginine-rich protein kinase family members (SRPKs)[14]. Treatment of
147 A549-ACE2 cells with increasing concentrations of SRPIN340 revealed significant toxicity
148 at a concentration of 160μM; lower concentrations however, were well tolerated (**Figure**
149 **1E**). We next infected cells treated with non-toxic concentrations of SRPIN340 with
150 SARS-CoV-2 and allowed multicycle viral growth for 24 hours. We observed a dramatic
151 SRPIN340-mediated decrease in viral RNA and infectious viral titer (up to 100,000-fold)
152 at the higher drug concentrations (**Figure 1F,G**).
153
154 The stronger viral inhibitory phenotype at higher concentrations of SRPIN340 suggested
155 that SRPK1 and SRPK2 (which are known to have similar substrate specificities[14,15]) likely
156 need to be inhibited simultaneously for full suppression of viral replication. To further test
157 that hypothesis, we made use of another small molecule (SPHINX31) that targets SRPK1
158 without appreciably affecting SRPK2[16]. Consistent with our previous data, while we could

159 significantly inhibit SARS-CoV-2 replication by targeting SRPK1 alone, the magnitude of
160 the effect was smaller than with SRPIN340 (**Supplemental Figure 2**). Finally, in order
161 to provide direct evidence that both SRPK1 and SRPK2 could indeed phosphorylate the
162 SARS-CoV-2 N protein, we performed *in vitro* phosphorylation assays with purified N,
163 SRPK1 or SRPK2, and γ32-P ATP. In a dose dependent manner, increasing
164 concentrations of the kinases led to increased N protein phosphorylation (**Figure 1H,I**).
165 Together, these data indicate that while SRPK1 is the dominant kinase (and thus most
166 enriched in the screen), SRPK2 likely provides at least partial redundancy for N
167 phosphorylation.
168
169 Since all of our experiments had been performed in our artificially generated A549-ACE2
170 cell lines, we next repeated the SRPIN340 inhibitor experiments in Calu-3 cells. Calu-3
171 is a human lung adenocarcinoma line that is naturally permissive to SARS-CoV-2
172 infection (**Figure 2A**). Toxicity of SRPIN340 in Calu-3 cells was similar to A549-ACE2
173 cells, and as expected, SARS-CoV-2 was significantly inhibited at the higher
174 concentrations of SRPIN340 (**Figure 2B-E**). After SRPIN340 treatment, the viral
175 replication intermediate double stranded RNA (dsRNA) became un-detectable,
176 expression of the viral S protein was significantly reduced, and viral RNA and cell free
177 infectious viral particles were reduced by more than three orders of magnitude (**Figure**
178 **2C-E, Supplemental Figure 3**).
179
180 N proteins of diverse human coronaviruses have highly conserved domains[17,18], including
181 the predicted SRPK1 phosphorylation sites (**Figure 2F, Supplemental Table 2**). We

182 therefore wanted to determine if the viral requirement for SRPK1/2 activity might be
183 broadly conserved as well. SRPIN340 treatment of cells infected with the
184 alphacoronavirus 229E (which is only distantly related to betacoronavirus SARS-CoV-2)
185 inhibited the virus by more than 1,000-fold at non-toxic concentrations of the drug (**Figure**
186 **2G-H**). These data indicate that the requirement for SRPK1/2 activity is not restricted to
187 SARS-CoV-2.
188
189 Finally, we wanted to understand the potential for targeting SARS-CoV-2 via inhibition of
190 SRPK1/2 in primary human lung cells. Type-2 pneumocytes isolated from four
191 independent healthy human donor lungs were first expanded in organoids embedded in
192 Matrigel (**Figure 2I**). For viral infection studies, pneumocytes were then cultured on
193 transwell membranes as monolayers. These distal alveolar cells were then treated with
194 drug or vehicle followed by infection with SARS-CoV-2. Viral replication (as measured by
195 viral protein staining) was strongly inhibited and reduced almost to the level of detection
196 (**Figure 2J,K**). Thus, the viral requirement for SRPK1/2 is not restricted to immortalized
197 cell lines and their kinase activities are essential for viral replication in some of the most
198 vulnerable populations of lung cells affected during severe COVID-19 disease[19].
199
200 **DISCUSSION**
201 Our screen for human host targets that could be pharmacologically inhibited to treat
202 COVID-19 disease identified SRPK1 and SRPK2 as kinases that are critical for the
203 replication of coronaviruses as divergent as 229E and SARS-CoV-2. SRPK1 and 2 are
204 expressed in most human tissues and have been implicated in a number of basal

205 processes including the regulation of transcript splicing and cellular stress responses[20,21].
206 Further, SRPK1 is upregulated in multiple cancers including prostate, breast, lung, and
207 glioma[22]. In particular, it is thought that its regulation of vascular endothelial growth factor
208 (VEGF) is central to its importance for a number of different diseases[23]. As such, a
209 number of different inhibitors of SRPK1 have been developed and used in various pre-
210 clinical disease models, however none of these compounds have yet been FDA
211 approved. In addition to its normal physiological roles and potential roles in cancer,
212 SRPK1/2 kinase activity has been previously reported as important for the replication of
213 a number of different viruses. These viruses include: hepatitis B virus, human
214 papillomavirus, hepatitis C virus, SARS-CoV, Ebola virus, human cytomegalovirus, and
215 herpes simplex virus-1[24-32]. While the mechanisms underlying how SRPK1/2 contribute
216 to the replication of these viruses differ, it is clear that many viruses have evolved to take
217 advantage of these host kinases.
218
219 One major question raised by our work is the relative contributions of different kinases to
220 SARS-CoV-2 viral protein phosphorylation. At least two recent reports have implicated
221 different kinases including: growth factor receptor (GFR) activated kinases, casein kinase
222 II (CK2), cyclin-dependent kinase (CDK), and protein kinase C (PKC) as generally
223 important, but not necessarily directly linked to N protein phosphorylation[12,13]. Previous
224 work with the related betacoronavirus SARS-CoV has shown that, at least in vitro, CDK,
225 glycogen synthase kinase (GSK), mitogen-activated protein kinase, SRPK1, and CK2 can
226 all phosphorylate the SARS-CoV N protein[32,33]. SRPK1 phosphorylation was reported to
227 affect ability of the SARS-CoV N protein to multimerize and inhibits host translation,

228 however any requirement for SRPK2, as well as effects on viral growth were not
229 reported[32]. Additionally, the growth of both SARS-CoV and mouse hepatitis virus (MHV)
230 have been reported to suppressed after treatment with GSK-3 inhibitors, presumably by
231 affecting N protein phosphorylation[34]. Further studies will be required to understand how
232 viral phosphorylation of SARS-CoV-2 protein affects their functions, as well as
233 experimentally define which kinases phosphorylate which viral proteins at which specific
234 locations. It will also be important to define potential kinase redundancy and the effects
235 on viral replication. At least for SARS-CoV-2, it appears that SRPK1/2 are central to the
236 regulation of viral infection, but it is worth noting that although our study has focused on
237 the phosphorylation of the N protein, we cannot rule out that the viral inhibition phenotype
238 observed is also or instead due to altered phosphorylation of other viral, or indeed host,
239 proteins.
240
241 Additionally, while we have provided data that SRPK1/2 inhibitors are effective in both
242 immortalized and primary cells, it remains unclear if targeting SRPK1/2 *in vivo* will have
243 a similar magnitude of effect. In support of potentially using SRPK1/2 inhibitors to treat
244 COVID-19 disease, several reports have utilized inhibitors of SRPK1 in animal models
245 and shown efficacy in suppressing phenotypes such as neovascular eye disease and
246 tumor growth, without apparent toxicity[16,35]. In conclusion, the development of safe and
247 efficacious anti-COVID-19 therapeutics is of the highest importance due to the ongoing
248 pandemic. Targeting of host factors essential for viral replication represents an approach
249 which may help to limit the emergence of viral resistance. Our study identified two host
250 kinases, against which inhibitors have already been developed and for which the

251 magnitude of inhibition of viral replication is on par with direct targeting of the viral
252 polymerase[36]. Continued development, optimization, and use of these kinase inhibitors
253 may lead to a class of host-directed antiviral therapeutics that could help combat the
254 current, and potentially future, coronavirus pandemics.
255

256 **MATERIALS AND METHODS**

257 Cell culture. All cells were obtained from ATCC and grown at 37°C in 5% CO_2. 293T and
258 A549 and Huh7 cells were grown in DMEM with 10% FBS, Glutamax, and
259 Penicillin/Streptomycin. VeroE6 cells were grown in MEM media supplemented with
260 Penicillin/Streptomycin, 10% FBS, 1 mM Pyruvate, and 1X MEM NEAA. Calu-3 cells
261 were grown in EMEM with 10% FBS and Penicillin/Streptomycin. Cells were selected in
262 0.5μg/ml Puromycin and 1μg/ml Blasticidin.
263

264 Plasmids. The ACE2-pLEX overexpression plasmid was generated by cloning a
265 synthesized gBlock of the ACE2 ORF (Ref. seq. NM_001371415.1) into the pLEX plasmid
266 via HiFi DNA Assembly (NEB Cat# M5520AA) and subsequent bacterial transformation.
267 Bacterial colonies were then selected and plasmid DNA isolated using the Genejet
268 Plasmid Miniprep kit (Thermo Fisher Cat# K0503). Plasmids were then sequenced via
269 Sanger sequencing to confirm successful cloning of the ACE2 ORF. Lentiviruses were
270 packaged as per standard protocols with a VSV-G envelope protein, A549-Cas9 cells
271 were transduced and selected with puromycin at 2μg/mL.
272

273 SARS-CoV-2 infections and titering

274 A stock of BEI isolate SARS-CoV-2 USA-WA1/2020 (kind gift of Greg Sempowski) was
275 grown on VeroE6 cells in viral growth media (MEM supplemented with 1% Pen/Strep, 2
276 % FBS, 1 mM Sodium Pyruvate, and 1x MEM NEAA). Infection was incubated for 1 hr
277 at 37℃. After infection total volume of media was brought to 30 mL. Virus was harvested
278 after 72 hrs of infection. To determine viral titer of stock and after drug treatment, a
279 monolayer of VeroE6 cells was infected with serially diluted virus for 1 hr. Virus was
280 removed and an agar overlay was added to each well (MEM, Penicillin/Streptomycin, 2%
281 FBS, 1 mM Pyruvate, 1x MEM NEAA, 0.3% Sodium Bicarbonate, Glutamax, 0.7% oxoid
282 agar). Plaque assays were incubated for 72 hrs then stained with either 0.1% Crystal
283 Violet in 10% Neutral Buffered Formalin or 0.05% Neutral Red. All viral infections took
284 place in cell specific media with only 2% FBS.
285
286 <u>HCoV-229E infections and titering</u>
287 A stock of isolate HCoV-229E VR-740 (ATCC) was grown on Huh7 cells in complete
288 media (DMEM supplemented with 10% FBS, 1% Pen/Strep, Glutamax). Infection was
289 incubated for 1hr at 37°C. After infection total volume of media was brought to 20 ml.
290 Virus was harvested after 36 hrs of infection. Viral titer of stock was determined via plaque
291 assay on Huh7 cells. A confluent monolayer of cells was infected with serial dilutions of
292 virus in complete media for 1 hr at 37°C. Virus was removed and an agar overlay was
293 added to each well (DMEM, 10% FBS, 1% Pen/Strep, Glutamax, 0.5% oxoid agar).
294 Plaque assays were incubated for 72 hrs then stained with 0.1% Crystal Violet in PBS.
295 Viral infection assays took place in complete media (DMEM, 10% FBS, 1% Pen/Strep,
296 Glutamax).

297

298 Quantitative Reverse Transcription PCR. Cells were resuspended in TRIzol Reagent
299 (Thermo Fisher Cat #15596018) and total RNA was isolated by either phase separation
300 with chloroform and isopropanol or using the Zymo Direct-zol RNA Miniprep kit (Zymo
301 Cat #R2050). One-step qRT-PCR was performed using the Invitrogen EXPRESS One-
302 Step Superscript qRT-PCR kit (Thermo Fisher Cat #11781200) and the commercial
303 Taqman probe ACE2 (Hs01085333_m1). The SARS-CoV2 primer/probe set were
304 synthesized using IDT DNA based on the sequences provided by the CDC "Research
305 Use Only 2019-Novel Coronavirus (2019-nCov) Real-time RT-PCR Primers and Probes"
306 set N1. For RNA extractions of 229E infected cells, RNA was extracted using NEB
307 Monarch total RNA miniprep kit (T2010S). To quantify viral RNA we used commercial
308 taqman probe CoV_229E (Vi06439671_s1). Reactions were cycled on the Applied
309 Biosystems QuantStudio 3 Real-Time PCR System and analyzed using QuantStudio
310 software version v1.4.1. RNA was normalized to the endogenous 18S primer-probe set
311 (Thermo Fisher Cat #4319413E).

312

313 Crystal violet staining

314 To visualize CPE of A549 cells expressing Ace2 or not, cells were infected with a MOI of
315 0.1 for 1 hr at 37℃. After 1 hr incubation 0.5 ml DMEM with 2% FBS was added to each
316 well and infection was allowed to continue for 72 hrs. After infection, the monolayer was
317 stained with 0.1% Crystal violet in 10% Neutral Buffered Formalin for 15 minutes. Stain
318 was then removed and cells were rinsed with ultra-pure water and then imaged.

319

320 CRISPR Screening and analysis

321 For the CRISPR screen, $2x10^7$ cells per replicate were transduced with CRISPR GeCKO
322 Library A lenti virus at a MOI of 0.8 in 7.5 ml DMEM with DEAE dextran. After 2 days,
323 cells were expanded and then seeded on day 4 post-transduction in 8 T75 plates per
324 replicate. Cells were infected at a MOI of 0.05 for 1 hr at 37℃. 10 ml of 2% DMEM was
325 added to the infection and cells were placed back in the incubator for 72 hrs. After
326 infection, cells were trypsinized, and centrifuged for 5 minutes at 500xg. Cells were
327 resuspended in DMEM with 10% FBS and replated in 4 T75 flasks. Cells grew for 48hrs
328 and then were expanded to 8 T75 flasks. The next day, 4 flasks of cells were collected
329 and the pellet was resuspended in DNA/RNA shield (Zymo Research). Genomic DNA
330 was purified using QiaAmp Blood Maxi (Qiagen). PCR was performed using Ex Taq DNA
331 Polymerase (Takara Cat #RR001) on 18.5 μg of genomic DNA. PCR bands were gel
332 purified using the GeneJet gel extraction kit (Thermo Scientific Cat #K0832). PCR
333 amplicons were quantified using an Agilent Bioanalyzer and samples were then
334 sequenced on an Illumina MiSeq. Raw reads were extracted and analyzed using the
335 MAGeCK pipeline[8]. Genes were ranked by the p-value assigned by MAGeCK.

336

337 SRPK inhibitor treatment assays

338 Two different inhibitors of SRPK1 and SRPK2 were used to assay effects on viral
339 replication, SRPIN340 and SPHINX31 (MedChem Express). Both drugs were suspended
340 in DMSO at 1000X the final concentration indicated. They were then diluted to the
341 indicated concentrations in cell specific media. Cells were treated with drug 12 hours
342 before infection. Cells were then infected for 1 hour as described above. After infection,

343 media with 2% FBS + drug or DMSO control was added to each well (qRT-PCR and Calu-
344 3 microscopy) or inoculum was removed and media with 2% FBS + drug or DMSO control
345 was added to each well (infectious titer quantification).
346
347 Cytotoxicity Assays. A549-Cas9 ACE2, Calu-3, or Huh7 cells were treated with the
348 indicated concentrations of SRPIN-340 or SPHINX-31 in a consistent volume of vehicle
349 (DMSO). 48 hours after treatment, samples were processed according to the CellTiter-
350 Glo (Promega) protocol and luminescence was determined using a luminometer.
351
352 Calu-3 Infection and immunofluorescence assays. For infections of Calu-3 cells for
353 immunofluorescence assays, cells were treated with DMSO or 53 μM SRPIN340 12 hrs
354 before infection. To infect Calu-3 cells media was removed and cells were washed with
355 0.5 mL PBS. Virus was added at MOI 2.5 and cells were infected at 37°C for 1 hr. After
356 infection, 200 μL media + 2x SRPIN340 or DMSO was added to cells and incubated at
357 37°C for 24 hrs. To fix cells, the culture plate was submerged in 10% neutral buffered
358 formalin for 2 hrs. NBF was removed and cells were placed in PBS. For immunostaining
359 cells were permeabilized with 0.1% Triton X-100 and blocked in PBS+ 5% BSA + 0.1%
360 Tween-20. Cells were stained with either an anti-dsRNA antibody (J2, Sigma
361 MABE1134) at a 1:125 dilution or an anti-SARS-CoV-2 Spike RBD protein (ProSci #9087)
362 at a 1:150 dilution. Alexa fluor 488 or 594 conjugated secondary antibodies were used at
363 a 1:1000 dilution. DNA was stained with Hoechst 33342 dye at a 1:10,000 dilution in
364 PBS. Images were taken on Bio-Rad Zoe fluorescent cell imager.
365

366 In vitro SRPK1/2 phosphorylation assays. To produce SARS-CoV-2 N protein, a 10 cm
367 plate of 293T cells were transfected with 15 μg of the pLVX-EF1alpha-nCOV2019-N-
368 2xStrep-IRES-Puro plasmid[12] using 45 μl Trans-IT LT1. 48 hrs post-transfection, cells
369 were lysed with 2 ml lysis buffer (50mM Tris pH 7.4, 150mM NaCl, 1% Triton X-100, 10%
370 Glycerol, cOmplete, EDTA-free protease inhibitor cocktail (Roche), PhosSTOP (Roche)
371 phosphatase inhibitor (1 tab per 10ml buffer)). Cellular debris was removed by
372 centrifugation 16,000xg for 5 minutes, and lysate was transferred to 2x 2ml tubes each
373 with 100 μl of Dynabeads Streptavidin M-280 (ThermoFisher) that were washed 1 time
374 with lysis buffer. Lysates rotated for 4 hrs at 4°C then beads were collected with a
375 magnet. The lysate was removed, and the beads were washed 3 times with 500 μl TBS
376 (50mM Tris pH 7.4, 150mM NaCl, EDTA-free protease inhibitor cocktail (Roche)). The 2
377 tubes of beads were combined and resuspended in 300μl TBS.
378
379 For kinase assays, N-bound beads were collected, and buffer was removed. The beads
380 were resuspended in 300 μl Kinase buffer (50 mM Tris pH7.4, 50 mM KCl, 5 mM $MgCl_2$,
381 1mM DTT) and 10 μl of beads+N or beads only were placed in 1.5 ml screw cap tubes.
382 1 ng, 10 ng, or 100 ng of SRPK1 or SRPK2 (ThermoFisher) were added to reactions as
383 well as Kinase buffer to bring total volume to 95 μl. Finally, ATP, [γ-32P]- 6000Ci/mmol
384 10mCi/ml was diluted 1:250 in Kinase buffer and 5μl of the diluted hot ATP (0.2 μCi) was
385 added to each reaction. Each reaction was done in triplicate and the reactions were
386 incubated at 30 degrees for 60 minutes with shaking. The samples were washed 3 x with
387 1 ml PBS (Gibco) and radioactivity incorporated was counted on a Beckman LS 6500
388 scintillation counter. The samples were then resuspended in loading dye and run on

389 BioRad Mini-PROTEAN TGX 4-20% stain-free gels. The gels were dried and radioactivity
390 visualized using Carestream BIOMAX MS film. A second gel was stained with
391 Coomassie Brilliant Blue to visualize bead bound proteins.
392
393 Bioinformatic prediction of SRPK1 phosphorylation sites. Sites predicted to be
394 phosphorylated by SRPK1 were identified using Group-based Prediction System v5.0[10]
395 and the following filter: Phosphorylation/Serine/threonine kinase/CMGC/SRPK/SRPK1.
396 Amino acid sequences from annotated ORFs in the following genbank accession
397 numbers (MN985325.1, NC_004718.3, JX869059.2, KF686340.1, MN306036.1,
398 KF530114.1, KF514433.1) were entered individually and a threshold of "high" was
399 applied. Only phosphorylation sites with a prediction score greater than the threshold of
400 71.312 were included in further analyses.
401
402 Human lung dissociation, primary type two pneumocytes purification, culturing, and
403 immunostaining. Human lung tissues were washed with PBS containing 1% Antibiotic-
404 Antimycotic and cut into small pieces. Then samples were digested with enzyme mixture
405 (Collagenase type I: 1.68 mg/ml, Dispase: 5U/ml, DNase: 10U/ml) at 37°C for 1h with
406 rotation. The cells were filtered through a 100 µm strainer, rinsed with 15 ml
407 DMEM/F12+10% FBS medium and centrifuged at 450x g for 10 min. The supernatant
408 was removed and the cell pellet was resuspended in red blood cell lysis buffer for 10min,
409 washed with DMEM/F12 containing 10% FBS and filtered through a 40 µm strainer. Total
410 cells were centrifuged at 450xg for 5 min at 4ºC and the cell pellet was processed for AT2
411 purification.

412

413 For human type two pneumocytes purification, approximately 2-10 million total human
414 lung cells were resuspended in MACS buffer and blocked with Human TruStain FcX
415 (Biolegend cat# 422032) for 15min at 4ºC followed by HTII-280 antibody (Terrace Biotech,
416 TB-27AHT2-280) staining for 1h at 4ºC. The cells were washed twice with MACS buffer
417 followed by incubation with anti-mouse IgM microbeads for 15 min at 4ºC. The cells were
418 loaded into the LS column and collected magnetically. AT2 cells ($3x10^3$) were
419 resuspended in serum free medium, mixed with an equal amount of Matrigel (Corning
420 Cat# 354230) and plated as drops on 6 well plates. The medium was changed every three
421 days. Alveolospheres were passaged every 14 days. For virus infection experiments
422 human AT2 cells were seeded at 10×10^4 cells per insert on 5% matrigel coated Transwell
423 with 0.4-µm pore-sized inserts (Corning). Cells were treated with DMSO or 53 µM
424 SRPIN340 12 hrs before infection with media on the top and bottom of transwell. To
425 infect cells, media was removed from top of transwell and cells were washed with 200 µl
426 PBS. Cells were then infected at a MOI of 1 for 1 hr. Virus was then removed, and cells
427 were cultured for 24 hrs. To fix cells and remove from BSL3, plates and wells were
428 submerged in 10% Neutral buffered formalin for 2 hrs. NBF was removed and cells were
429 placed in PBS until staining.

430

431 For immunostaining of the cultures, the membrane from the transwell insert was cut
432 out with a scalpel and washed with PBS, permeabilized in PBST (0.1% Triton X-100 in
433 PBS), and incubated with blocking buffer (1% BSA in PBST) for 1h at room temperature.
434 Samples were incubated with primary antibodies: Prosurfactant protein C (1:500,

435 Milipore, cat# AB3786) and SARS-CoV-2 (1:500, Genetex cat# GTX632604) in blocking
436 buffer at 4°C overnight. Membranes were then washed 3 times in PBST, incubated with
437 secondary antibodies in blocking buffer for 1h at room temperature followed be three
438 washes with PBST and mounted using Fluor G reagent with DAPI. All confocal images
439 were collected using Olympus Confocal Microscope FV3000 using a 40X objectives.
440

441 **ACKNOWLEDGMENTS**

442 The authors would like to acknowledge experimental support from, and helpful discussion
443 with, Hal Bogerd and Bryan Cullen. NSH is partially funded by the Defense Advanced
444 Research Projects Agency's (DARPA) PReemptive Expression of Protective Alleles and
445 Response Elements (PREPARE) program (Cooperative agreement #HR00111920008).
446 The views, opinions and/or findings expressed are those of the authors and should not
447 be interpreted as representing the official views or policies of the U.S. Government. JDT
448 was partially supported by T32-CA009111. The following reagent was deposited by the
449 Centers for Disease Control and Prevention and obtained through BEI Resources, NIAID,
450 NIH: SARS-Related Coronavirus 2, Isolate USA-WA1/2020, NR-52281. Biocontainment
451 work was performed in the Duke Regional Biocontainment Laboratory, which received
452 partial support for construction from the National Institutes of Health, National Institute of
453 Allergy and Infectious Diseases (UC6-AI058607).
454

455 **DISCLOSURES**

456 Duke University has filed for intellectual property protection regarding the use of SRPK
457 inhibitors in the treatment of COVID-19.

458 **REFERENCES**

459 1 Yuki, K., Fujiogi, M. & Koutsogiannaki, S. COVID-19 pathophysiology: A review.
460 *Clin Immunol* **215**, 108427, doi:10.1016/j.clim.2020.108427 (2020).

461 2 Li, Q. *et al.* Early Transmission Dynamics in Wuhan, China, of Novel
462 Coronavirus-Infected Pneumonia. *N Engl J Med* **382**, 1199-1207,
463 doi:10.1056/NEJMoa2001316 (2020).

464 3 Gordon, C. J. *et al.* Remdesivir is a direct-acting antiviral that inhibits RNA-
465 dependent RNA polymerase from severe acute respiratory syndrome coronavirus
466 2 with high potency. *J Biol Chem* **295**, 6785-6797,
467 doi:10.1074/jbc.RA120.013679 (2020).

468 4 Beigel, J. H. *et al.* Remdesivir for the Treatment of Covid-19 - Preliminary Report.
469 *N Engl J Med*, doi:10.1056/NEJMoa2007764 (2020).

470 5 Wei, J. *et al.* Genome-wide CRISPR screen reveals host genes that regulate
471 SARS-CoV-2 infection. *bioRxiv*, doi:doi.org/10.1101/2020.06.16.155101 (2020).

472 6 Harcourt, J. *et al.* Severe Acute Respiratory Syndrome Coronavirus 2 from
473 Patient with Coronavirus Disease, United States. *Emerg Infect Dis* **26**, 1266-
474 1273, doi:10.3201/eid2606.200516 (2020).

475 7 Sanjana, N. E., Shalem, O. & Zhang, F. Improved vectors and genome-wide
476 libraries for CRISPR screening. *Nat Methods* **11**, 783-784,
477 doi:10.1038/nmeth.3047 (2014).

478 8 Li, W. *et al.* MAGeCK enables robust identification of essential genes from
479 genome-scale CRISPR/Cas9 knockout screens. *Genome Biol* **15**, 554,
480 doi:10.1186/s13059-014-0554-4 (2014).

481 9 Cohen, P. Protein kinases--the major drug targets of the twenty-first century? *Nat*
482 *Rev Drug Discov* **1**, 309-315, doi:10.1038/nrd773 (2002).

483 10 Wang, C. *et al.* GPS 5.0: An Update on the Prediction of Kinase-specific
484 Phosphorylation Sites in Proteins. *Genomics Proteomics Bioinformatics* **18**, 72-
485 80, doi:10.1016/j.gpb.2020.01.001 (2020).

486 11 Davidson, A. D. *et al.* Characterisation of the transcriptome and proteome of
487 SARS-CoV-2 reveals a cell passage induced in-frame deletion of the furin-like
488 cleavage site from the spike glycoprotein. *Genome Med* **12**, 68,
489 doi:10.1186/s13073-020-00763-0 (2020).

490 12 Bouhaddou, M. *et al.* The Global Phosphorylation Landscape of SARS-CoV-2
491 Infection. *Cell* **182**, 685-712 e619, doi:10.1016/j.cell.2020.06.034 (2020).

492 13 Klann, K. *et al.* Growth factor receptor signaling inhibition prevents SARSCoV-2
493 replication. *bioRxiv*, doi:doi.org/10.1101/2020.05.14.095661 (2020).

494 14 Fukuhara, T. *et al.* Utilization of host SR protein kinases and RNA-splicing
495 machinery during viral replication. *Proc Natl Acad Sci U S A* **103**, 11329-11333,
496 doi:10.1073/pnas.0604616103 (2006).

497 15 Wang, H. Y. *et al.* SRPK2: a differentially expressed SR protein-specific kinase
498 involved in mediating the interaction and localization of pre-mRNA splicing
499 factors in mammalian cells. *J Cell Biol* **140**, 737-750, doi:10.1083/jcb.140.4.737
500 (1998).

501 16 Batson, J. *et al.* Development of Potent, Selective SRPK1 Inhibitors as Potential
502 Topical Therapeutics for Neovascular Eye Disease. *Acs Chem Biol* **12**, 825-832,
503 doi:10.1021/acschembio.6b01048 (2017).

504 17 Chen, C. Y. *et al.* Structure of the SARS coronavirus nucleocapsid protein RNA-
505 binding dimerization domain suggests a mechanism for helical packaging of viral
506 RNA. *J Mol Biol* **368**, 1075-1086, doi:10.1016/j.jmb.2007.02.069 (2007).

507 18 McBride, R., van Zyl, M. & Fielding, B. C. The Coronavirus Nucleocapsid Is a
508 Multifunctional Protein. *Viruses-Basel* **6**, 2991-3018, doi:10.3390/v6082991
509 (2014).

510 19 Mason, R. J. Pathogenesis of COVID-19 from a cell biology perspective. *Eur*
511 *Respir J* **55**, doi:10.1183/13993003.00607-2020 (2020).

512 20 Aubol, B. E., Jamros, M. A., McGlone, M. L. & Adams, J. A. Splicing kinase
513 SRPK1 conforms to the landscape of its SR protein substrate. *Biochemistry* **52**,
514 7595-7605, doi:10.1021/bi4010864 (2013).

515 21 Zhong, X. Y., Ding, J. H., Adams, J. A., Ghosh, G. & Fu, X. D. Regulation of SR
516 protein phosphorylation and alternative splicing by modulating kinetic interactions
517 of SRPK1 with molecular chaperones. *Genes Dev* **23**, 482-495,
518 doi:10.1101/gad.1752109 (2009).

519 22 Bullock, N. & Oltean, S. The many faces of SRPK1. *J Pathol* **241**, 437-440,
520 doi:10.1002/path.4846 (2017).

521 23 Oltean, S. *et al.* SRPK1 inhibition in vivo: modulation of VEGF splicing and
522 potential treatment for multiple diseases. *Biochem Soc Trans* **40**, 831-835,
523 doi:10.1042/BST20120051 (2012).

524 24 Takamatsu, Y. *et al.* Serine-Arginine Protein Kinase 1 Regulates Ebola Virus
525 Transcription. *mBio* **11**, doi:10.1128/mBio.02565-19 (2020).

526 25 Karakama, Y. *et al.* Inhibition of hepatitis C virus replication by a specific inhibitor
527 of serine-arginine-rich protein kinase. *Antimicrob Agents Chemother* **54**, 3179-
528 3186, doi:10.1128/AAC.00113-10 (2010).

529 26 Gaddy, C. E., Wong, D. S., Markowitz-Shulman, A. & Colberg-Poley, A. M.
530 Regulation of the subcellular distribution of key cellular RNA-processing factors
531 during permissive human cytomegalovirus infection. *J Gen Virol* **91**, 1547-1559,
532 doi:10.1099/vir.0.020313-0 (2010).

533 27 Prescott, E. L. *et al.* Human papillomavirus type 1 E1^E4 protein is a potent
534 inhibitor of the serine-arginine (SR) protein kinase SRPK1 and inhibits
535 phosphorylation of host SR proteins and of the viral transcription and replication
536 regulator E2. *J Virol* **88**, 12599-12611, doi:10.1128/JVI.02029-14 (2014).

537 28 Tunnicliffe, R. B. *et al.* Molecular Mechanism of SR Protein Kinase 1 Inhibition by
538 the Herpes Virus Protein ICP27. *mBio* **10**, doi:10.1128/mBio.02551-19 (2019).

539 29 Zheng, Y. Y., Fu, X. D. & Ou, J. H. J. Suppression of hepatitis B virus replication
540 by SRPK1 and SRPK2 via a pathway independent of the phosphorylation of the
541 viral core protein. *Virology* **342**, 150-158, doi:10.1016/j.virol.2005.07.030 (2005).

542 30 Heger-Stevic, J., Zimmermann, P., Lecoq, L., Bottcher, B. & Nassal, M. Hepatitis
543 B virus core protein phosphorylation: Identification of the SRPK1 target sites and
544 impact of their occupancy on RNA binding and capsid structure. *Plos Pathog* **14**,
545 doi:ARTN e1007488
546 10.1371/journal.ppat.1007488 (2018).

547 31 Daub, H. *et al.* Identification of SRPK1 and SRPK2 as the major cellular protein
548 kinases phosphorylating hepatitis B virus core protein. *J Virol* **76**, 8124-8137,
549 doi:10.1128/Jvi.76.16.8124-8137.2002 (2002).

550 32 Peng, T. Y., Lee, K. R. & Tarn, W. Y. Phosphorylation of the arginine/serine
551 dipeptide-rich motif of the severe acute respiratory syndrome coronavirus
552 nucleocapsid protein modulates its multimerization, translation inhibitory activity
553 and cellular localization. *FEBS J* **275**, 4152-4163, doi:10.1111/j.1742-
554 4658.2008.06564.x (2008).

555 33 Surjit, M. *et al.* The severe acute respiratory syndrome coronavirus nucleocapsid
556 protein is phosphorylated and localizes in the cytoplasm by 14-3-3-mediated
557 translocation. *J Virol* **79**, 11476-11486, doi:10.1128/Jvi.79.17.11476-11486.2005
558 (2005).

559 34 Wu, C. H. *et al.* Glycogen synthase kinase-3 regulates the phosphorylation of
560 severe acute respiratory syndrome coronavirus nucleocapsid protein and viral
561 replication. *J Biol Chem* **284**, 5229-5239, doi:10.1074/jbc.M805747200 (2009).

562 35 Mavrou, A. *et al.* Serine-arginine protein kinase 1 (SRPK1) inhibition as a
563 potential novel targeted therapeutic strategy in prostate cancer. *Oncogene* **34**,
564 4311-4319, doi:10.1038/onc.2014.360 (2015).

565 36 Sheahan, T. P. *et al.* An orally bioavailable broad-spectrum antiviral inhibits
566 SARS-CoV-2 in human airway epithelial cell cultures and multiple coronaviruses
567 in mice. *Sci Transl Med* **12**, doi:10.1126/scitranslmed.abb5883 (2020).
568
569
570
571

572 **MAIN FIGURES AND LEGENDS**

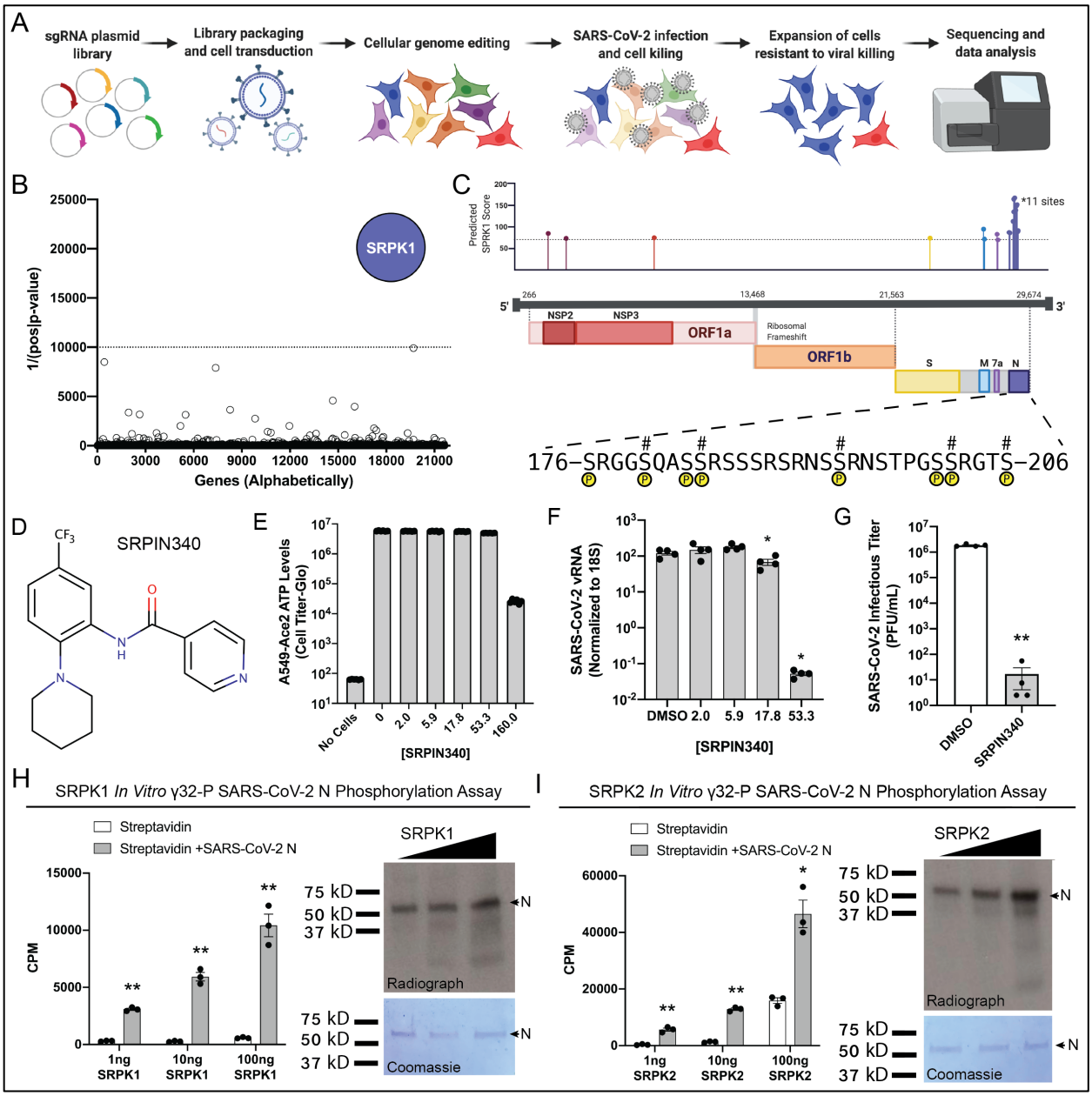

573

574 **Figure 1. CRISPR screening identifies SRPK1/2 as kinases that mediate**
575 **phosphorylation of the SARS-CoV-2 N protein.** (a) Diagram of CRISPR GeCKO
576 screen in A549-Cas9-Ace2 cells with SARS-CoV-2. (b) Representation of predicted hits
577 from the CRISPR screen. Genes are arranged on x-axis alphabetically and y-axis score
578 is inverse of the p-value for enriched genes. Genes with p-values of less than 10^{-4} were

579 represented with larger dots and the gene name. (c) Map of the SARS-CoV-2 genome
580 with potential SRPK1 phosphorylation sites indicated in graph on the top. Zoom-in of
581 amino acids 176-204 of the N protein that contain multiple potential SRPK1
582 phosphorylation sites. # above the amino acids indicate predicted SRPK1
583 phosphorylation sites while the yellow circles bellow the amino acids indicate the serines
584 reported to be phosphorylated by both Davidson et al. and Bouhaddou et al.[11,12]. (d)
585 Chemical structure of SRPIN340. (e) CellTiter-GLO assay in A549-Cas9-Ace2 cells (n=6)
586 determining the toxicity of SRPIN340 at multiple concentrations of drug. (f) After
587 treatment of A549-Cas9-Ace2 cells with different concentrations of SRPIN 340, SARS-
588 CoV-2 mRNA (n=4) was quantified by qRT-PCR. (g) Infectious virus was quantified (n=4)
589 by plaque assay 48 hrs after infection of A549-Cas9-Ace2 cells that were treated with
590 DMSO or 53 μM SRPIN340. (h) *In vitro* phosphorylation assay using purified SRPK1
591 protein and SARS-CoV-2 N protein on streptavidin beads or streptavidin beads only as
592 substrate. On the left CPM were quantified after phosphorylation reaction, n=3. On the
593 right top panel radiograph of phosphorylated N protein, on the bottom panel Coomassie
594 stained gel showing equal loading of N protein. (i) *In vitro* phosphorylation assay using
595 purified SRPK2 protein and SARS-CoV-2 N protein on streptavidin beads or streptavidin
596 beads only as substrate. On the left CPM were quantified after phosphorylation reaction,
597 n=3. On the right top panel radiograph of phosphorylated N protein, on the bottom panel
598 Coomassie stained gel showing equal loading of N protein. All experiments are
599 representative of at least two independent biological replicates. In all panels, error bars
600 represent SEM, *$p<0.05$ **$p<0.001$ by an unpaired, student's t-test
601

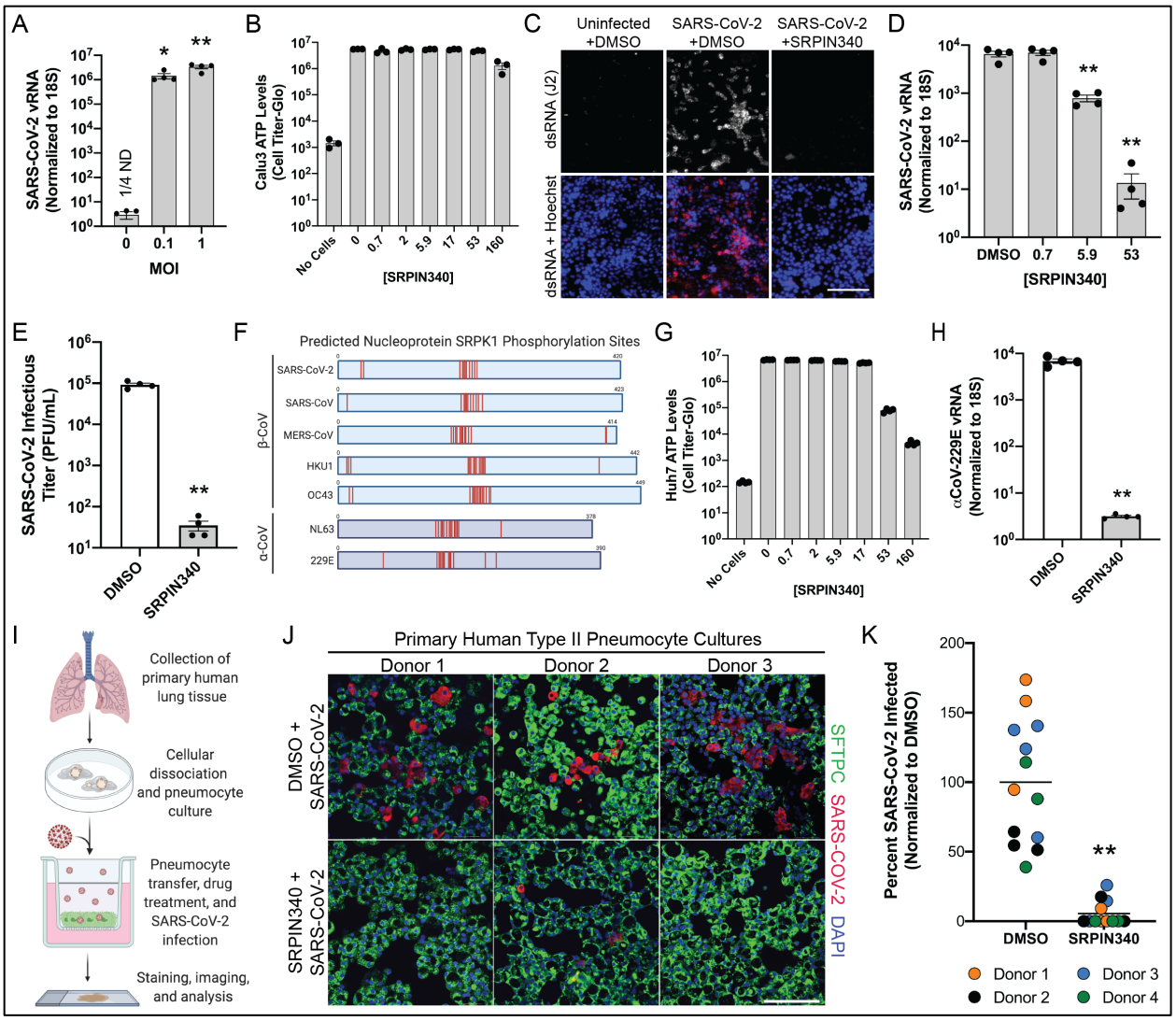

Figure 2. Pharmacological inhibition of SRPK1/2 compromises the replication of multiple human coronaviruses. (a) Quantification of SARS-CoV-2 mRNA by qRT-PCR after infection of Calu-3 cells at different MOIs n=4. (b) CellTiter-Glo assay in Calu-3 cells determining the toxicity of SRPIN340 at multiple concentrations of drug n=3. (c) Calu-3 cells were uninfected or infected with SARS-CoV-2, MOI=2.5 after treatment with DMSO control or 53 μM SRPIN340. DNA was stained with Hoechst (blue) and dsRNA stained with J2 antibody (red). Scale bar represents 150 μm. (d) Calu-3 cells were treated with DMSO control or different concentrations of SRPIN340 then infected with MOI 0.005.

611 SARS-CoV-2 mRNA was quantified by qRT-PCR n=4. (e) Calu-3 cells were treated with
612 DMSO control or 53 μM SRPIN340 then infected with MOI 0.01 for 48 hrs. Infectious
613 virus was quantified by plaque assay n=4. (f) Diagram of the N protein of multiple
614 coronaviruses. Red lines within protein indicate predicted SRPK1 phosphorylation sites.
615 (g) Huh7 cells were treated with different concentrations of SRPIN340 and cytotoxicity
616 was assayed with the CellTiter-Glo assay n=4. (h) Huh7 cells were treated with DMSO
617 or 17 μM SRPIN340 then infected with 229E MOI 0.01. Viral RNA was quantified with
618 qRT-PCR n=4. (i) Diagram of primary type II pneumocyte cell culturing and infections.
619 (j) Primary type II pneumocytes were isolated from different donors, cultured on transwell
620 membranes, treated with DMSO or 53 μM SRPIN340 and then infected at MOI=1. After
621 24 hrs cells were fixed and stained for type II marker SFTPC (green), DAPI (blue) or
622 SARS-CoV-2 (red). Scale bar= 100 μm. (k) Microscopy images from (j) were quantified
623 and % positive cells from four independent donors were plotted, $n \geq 3$. For all panels, error
624 bars represent SEM and *$p<0.05$ **$p<0.001$ by an unpaired, student's t-test.
625